Hindawi
Advances in Civil Engineering
Volume 2020, Article ID 8863181, 11 pages
https://doi.org/10.1155/2020/8863181

Research Article

Predicting the Permeability of Pervious Concrete Based on the Beetle Antennae Search Algorithm and Random Forest Model

Jiandong Huang,[1,2] Tianhong Duan ,[1,2] Yi Zhang ,[3] Jiandong Liu,[1] Jia Zhang,[2] and Yawei Lei[4]

[1]*State Key Laboratory of Coal Resources and Safe Mining, China University of Mining and Technology, Xuzhou 221116, China*
[2]*School of Mines, China University of Mining and Technology, Xuzhou 221116, China*
[3]*Key Laboratory of Road and Traffic Engineering of the Ministry of Education, College of Transportation Engineering, Tongji University, 4800 Caoan Road, Shanghai 201804, China*
[4]*China Construction Second Engineering Bureau Ltd., Beijing 100160, China*

Correspondence should be addressed to Tianhong Duan; passionduan@cumt.edu.cn and Yi Zhang; zhangyi1990@tongji.edu.cn

Received 16 September 2020; Revised 30 October 2020; Accepted 6 December 2020; Published 29 December 2020

Academic Editor: Junfei Zhang

Pervious concrete is an environmentally friendly material that improves water permeability, skid resistance, and sound absorption characteristics. Permeability is the most important functional performance for the pervious concrete while limited studies have been conducted to predict permeability based on mix-design parameters. This study proposed a method to combine the beetle antennae search (BAS) and random forest (RF) algorithm to predict the permeability of pervious concrete. Based on the 36 samples designed in the laboratory and 4 key influencing variables, the permeability of pervious concrete can be obtained by varying mix-design parameters by RF. BAS algorithm was used to tune the hyperparameters of RF, which were then verified by the so-called 10-fold cross-validation. Furthermore, the model to combine the BAS and RF was validated by the correlation parameters. The results showed that the hyperparameters of RF can be tuned by the BAS efficiently; the BAS can combine the conventional RF algorithm to construct the evolved model to predict the permeability of pervious concrete; the cement/aggregate ratio was the most significant variable to determine the permeability, followed by the coarse aggregate proportions.

1. Introduction

Pervious concrete is similar to conventional concrete but designed without fine aggregates (i.e., sand) and has a porosity and median pore diameter in the range of 0.15–0.3 and 2–4 mm, respectively [1–4]. Pervious concrete is an environmentally friendly material that improves skid resistance and sound absorption characteristics and reduces the "heat island effect" [5–10]. Further, pervious concrete displays better water permeability characteristics due to connected pore structure through the fluid [2, 11].

Permeability is the most important functional performance for the pervious concrete, and it has been confirmed to be closely related to the pore structure, which determines the permeation rate per unit area. The permeability is traditionally characterized by the so-called permeability coefficient, and its value is typically between 0.1 and 2 cm/s [12, 13]. According to whether it is directly related to permeability performance of pervious concrete, pore-structure parameters can be divided into two categories: nonconnected related parameters and connected related parameters. Nonconnected related parameters include total porosity, pore diameter, and distribution, and connected related parameters include connected porosity and pore tortuosity [14–16]. The total porosity of pervious concrete can be defined as the ratio of the voids volume to the specimen volume, which mainly depends on the ratio of mortar to aggregate and the compactness degree of the concrete, usually between 15% and 25% [17]. Studies have shown that the total porosity of pervious concrete decreases with the increase of the ratio of mortar to aggregate [18]. Besides, as the pressure load or vibration load increases, the

skeleton of pervious concrete tends to be dense, and the total porosity gradually decreases [19]. Connected porosity is also called effective porosity, that is, pores that can effectively pass air and liquid. Cosic et al. used X-ray tomography technology to study the effects of aggregate type and size on the pore structure and found that the interconnected porosity is a function of aggregate size, accounting for about 50% to 70% of the total porosity [20]. Also, another study confirmed that the connected porosity decreases with the increase of the amount of mortar [13]. Kuang et al. defined the ratio of the effective length of the pore to the total length of the pervious concrete specimen as the pore tortuosity, which can more intuitively reflect the characteristics of the pore structure [21]. Zhong et al. defined the pore tortuosity as a function of the average pore diameter and the aggregate size and believed that the fluidity of the mortar and the aggregate size directly affects the pore tortuosity. The pore tortuosity increases with the decrease of aggregate size and the increase of mortar fluidity [22]. It can be confirmed from the previous research that the parameters affecting the permeability of pervious concrete have been studied, including aggregate size and mortar content [14, 17, 19]. However, from the author's knowledge, few studies can predict the water permeability based on these variable parameters. Although some studies can propose models for predicting permeability from a microscopic perspective (pore structure, the effective length of pores, etc.) [21, 22], these models often require the acquisition of concrete cross-section information firstly (e.g., CT scan), and it is difficult to predict from the perspective of mixture design. Therefore, systematical investigations are required to evaluate the permeability of pervious concrete in a way of more economic and efficient technology as per the permeability database including varying parameters.

Machine learning methods are gradually applied to the evaluation and prediction of the mechanical performance of cement materials [22–32]. The punching shear capacity of steel fiber reinforced concrete slabs was predicted by using the sequential piecewise multiple linear regression and artificial neural network [33]. Jamal et al evaluated the possibility to predict the strength of recycled aggregate concrete using machine learning methods, multiple linear regression, and adaptive neurofuzzy inference system [34]. The same method was also used by Khademi et al. in a follow-up study for the prediction of compressive strength after 28 days [35]. In the above-mentioned methods, the agreement between the experimental results and the predicted results indicates the feasibility of the machine learning algorithm for strength prediction of cement materials. However, within the scope of the author's knowledge, the limited literature can provide accurate and widely used machine learning algorithms specifically for the functional performance (permeability, workability, etc.) of cement materials.

Furthermore, the above machine learning methods have been used for the specific predictions in cement-based materials, but limitations still existed in these studies, such as uncertain structure, time-consuming, and low efficiency. Consequently, more efficient and simple machine learning models need to be proposed and used to predict the permeability of pervious concrete. In recent years, due to the good performance of the random forest (RF) method in nonlinear regression and classification, it has been used to predict the mechanical and functional properties of concrete. Specifically, the coefficients of thermal expansion and other properties of concrete were confirmed to be accurately predicted using the RF method [36]. The same method was also employed to predict and evaluate the compressive strength of high-performance concrete. However, no corresponding studies were reported to use RF to predict the permeability of pervious concrete so far. Besides, as far as the RF model employed in the previous studies, the hyperparameters were still required to be optimized to arrive at their optimized predictive ability [37].

2. Research Objective and Overview

The present study aims to propose a robust machine learning technique to be used as a tool to predict the permeability of pervious concrete. An efficient global optimization algorithm (called the beetle antennae search, BAS) proposed by Jiang et al. was adopted in this study to obtain the optimized parameters of RF [37]. In this way, the random forest (RF) and beetle antennae search (BAS) algorithms were combined to build a robust machine learning technique, named as BRF method. To plant the database applied to the proposed BRF method, varying mixes of pervious concrete were designed considering four parameters (aggregate proportion %: 9.5~13.2 mm; aggregate proportion: 4.75~9.5 mm; aggregate proportion %: 2.36~4.75 mm; cement-aggregate ratio) that have significant effects on the permeability coefficient according to the investigation based on known literature. Using the obtained database of the permeability of the pervious concrete, the training subset and the testing subset were developed for machine learning, and finally, the prediction of permeability can be realized. The above research process can be overviewed in Figure 1.

3. Methodology

3.1. BRF Model. BRF model combines BAS and RF, where RF is used to determine the nonlinear relationship of the dataset, and BAS is applied to adjust the hyperparameters of RF. The detailed introduction for the BRF model is described as follows.

3.1.1. Random Forest (RF) Model. The RF model is a modeling method that combines multiple independent classification trees. The algorithm can improve the prediction accuracy on the premise that the calculation is not significantly increased. The principle framework of the RF model is presented in Figure 2.

RF is a classifying method that uses a collection of classification trees, and every classification tree is constructed by using guided samples of data. For the tree construction, variables are randomly selected in each partition as the candidate variable set.

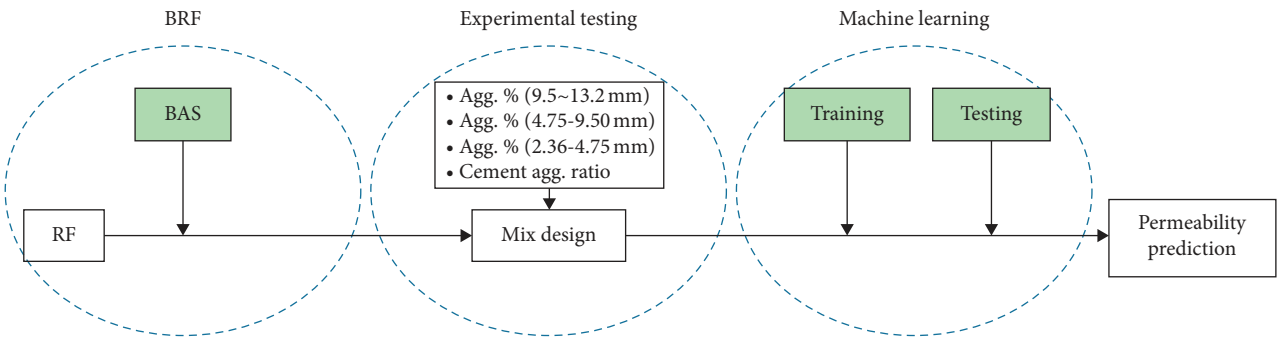

Figure 1: Research overview.

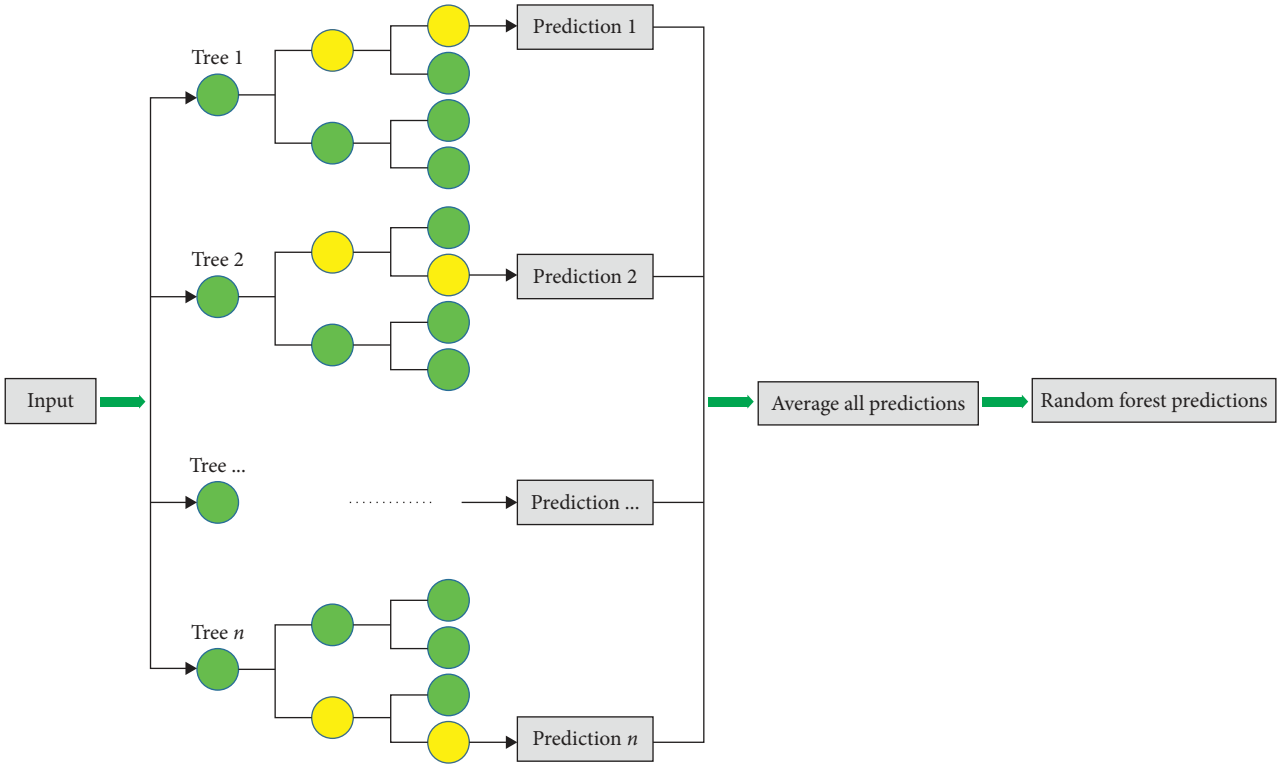

Figure 2: Principle of the RF model.

3.1.2. Beetle Antennae Search (BAS). The design of the BAS algorithm is inspired by the behavior of the beetle when looking for a mate. Similar to intelligent optimization algorithms such as genetic algorithm, particle swarm algorithm, and simulated annealing, BAS does not need to know the specific form of the function and does not need gradient information to achieve efficient optimization. Compared with the particle swarm algorithm, BAS only requires one individual, that is, a long beetle, which greatly reduces the amount of calculation. It simulates the behavior of beetles, which can use the two antennae to randomly explore nearby areas and transform them into a higher concentration of odor. The performance of the BAS algorithm has been evaluated in various applications [39, 40]. Figure 3 gives the work chart of the BAS algorithm.

4. Experimental Testing and Model Validation

4.1. Experimental Testing. The purpose of the laboratory testing is to evaluate the influence of different variables in the design of pervious concrete on the permeability coefficient and then provide enough data to be assembled as the training set and testing set. The raw materials, mixture design, sample preparation, and permeability test methods used in the laboratory testing are introduced as follows.

4.1.1. Raw Materials. Cement and aggregate were used as the raw materials to prepare the pervious concrete specimen. The ordinary Portland cement grade 42.5 was selected as the cemented material. Table 1 gives the physical properties of the cement.

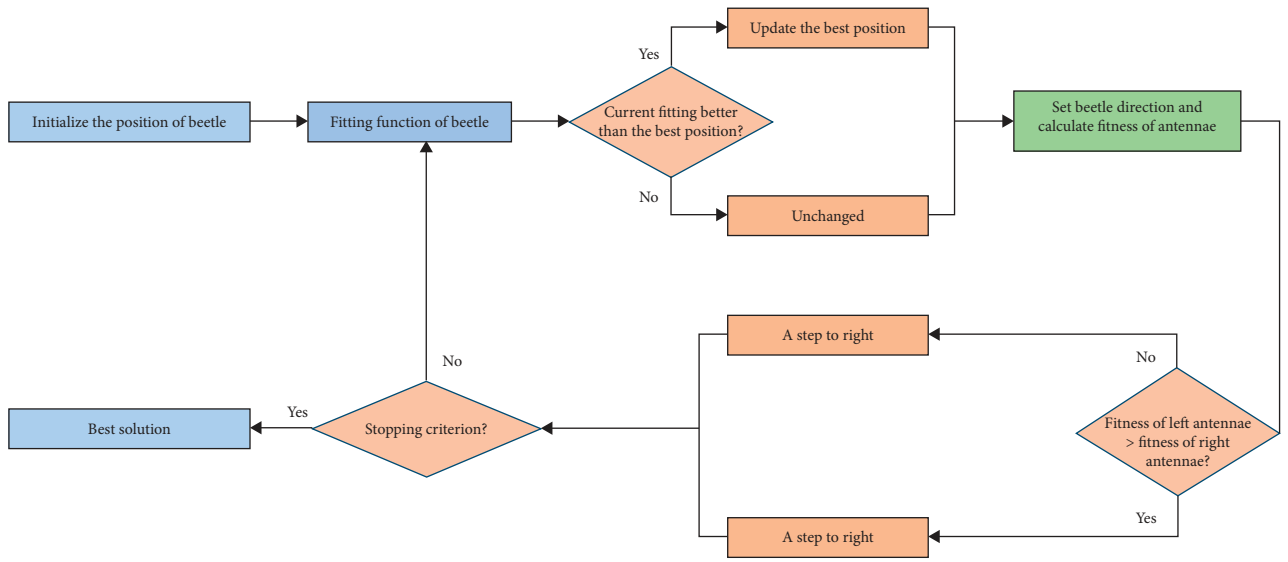

Figure 3: Work chart of the BAS algorithm.

Table 1: Physical properties of the cement.

Coagulation time (min)		Flexural strength (MPa)		Compressive strength (MPa)	
Initial solidification	Finial solidification	3d	28d	3d	28d
165	330	5.1	7.1	20.9	44.3

Table 2: Physical properties of coarse aggregate.

Aggregates	Size (mm)	Apparent density (kg/m^3)	Bulk density (kg/m^3)
G_1	2.36–4.75	2787	1406
G_2	4.75–9.50	2844	1513
G_3	9.50–13.2	2840	1537

According to the standard CJJ/T135-200, four different sizes of limestone gravel aggregates (G_1, G_2, and G_3) were adopted in the present study. The physical indexes are given in Table 2. To ensure that the performance of the prepared pervious concretes to meet the requirements, the aggregate used should be placed in a constant temperature oven in advance to keep it clean and dry. A liquid modifier for the pervious concrete provided by a local supplier in Jiangsu Province was used.

4.1.2. Mix Design and Sample Preparation. To evaluate the effects of different variables on the permeability coefficient, the designed mix was divided into 69 groups according to different aggregate proportions and cement-aggregate ratio (C/A), as shown in Table 3.

Generally, the reasonable water-cement ratio (W/C) of pervious concrete ranges from 0.29 to 0.33, and 0.3 was determined in the present study for the mixing [7]. Three possible C/A values (0.22, 0.24, and 0.26) were chosen to determine their effects on water permeability, based on the results of previous studies conducted [18, 39, 40]. After stirring and weighing, the mixture of pervious concrete was poured into a cylindrical mold with a diameter of 100 mm and a thickness of 50 mm to obtain samples for permeability testing. Before demolding, cover the sample and mold with damp geotextile in the laboratory at a temperature of 20°C for 24 h. Then, the samples were placed in a standard curing room with a temperature of 20°C and humidity of 95% for 28 days. It should be noted that three replicate samples were prepared for each mixture to reduce the deviation.

4.1.3. Experimental Methods. As far as the permeability testing methods concerned, the falling-head and constant-head method were typically used in the previous studies [41, 42]. For materials with poor permeability (permeability coefficient $< 10^{-3}$ cm/s) such as cohesive soil and fine-grained soil, permeability is typically measured by the falling-head method since the flow is too small to be measured. However, for pervious concrete, its permeability coefficient is relatively high (>0.35 cm/s) and the constant-head method is more suitable to measure the permeability coefficient. Therefore, the constant-head method was selected for the determination of the permeability coefficient in the study. The permeability coefficient was determined based on Darcy's law, where the amount of water passing through the concrete per unit time is proportional to the surface area and inversely proportional to the length of the permeable path, as given in equation (1):

$$k_t = \frac{Q \cdot D}{A \cdot H \cdot \Delta t}, \quad (1)$$

where k_t (mm/s) represents the coefficient of permeability at the given temperature t (°C), Q (mm^3) is the amount of water flowing through concrete in Δt (s) time; D (mm) and A (mm^2) are the thickness and area of the pervious concrete

Table 3: Mix proportions.

Mixes	Aggregate proportion			Cement-aggregate ratio (C/A)	Water-cement ratio
	G_1	G_2	G_3		
M1	1	0	0	0.22	
M2	1	0	0	0.24	
M3	1	0	0	0.26	
M4	0	1	0	0.22	
M5	0	1	0	0.24	
M6	0	1	0	0.26	
M7	0	0	1	0.22	
M8	0	0	1	0.24	
M9	0	0	1	0.26	
M10	0.1	0.9	0	0.22	
M11	0.1	0.9	0	0.24	
M12	0.1	0.9	0	0.26	
M13	0.2	0.8	0	0.22	
M14	0.2	0.8	0	0.24	
M15	0.2	0.8	0	0.26	
M16	0	0.9	0.1	0.22	
M17	0	0.9	0.1	0.24	
M18	0	0.9	0.1	0.26	
M19	0	0.8	0.2	0.22	
M20	0	0.8	0.2	0.24	
M21	0	0.8	0.2	0.26	
M22	0.1	0.8	0.1	0.22	
M23	0.1	0.8	0.1	0.24	
M24	0.1	0.8	0.1	0.26	
M25	0.1	0.7	0.2	0.22	
M26	0.1	0.7	0.2	0.24	
M27	0.1	0.7	0.2	0.26	
M28	0.1	0.6	0.3	0.22	
M29	0.1	0.6	0.3	0.24	
M30	0.1	0.6	0.3	0.26	
M31	0.1	0.5	0.4	0.22	
M32	0.1	0.5	0.4	0.24	
M33	0.1	0.5	0.4	0.26	
M34	0.1	0.4	0.5	0.22	
M35	0.1	0.4	0.5	0.24	0.3
M36	0.1	0.4	0.5	0.26	
M37	0.15	0.7	0.15	0.22	
M38	0.15	0.7	0.15	0.24	
M39	0.15	0.7	0.15	0.26	
M40	0.15	0.6	0.25	0.22	
M41	0.15	0.6	0.25	0.24	
M42	0.15	0.6	0.25	0.26	
M43	0.15	0.5	0.35	0.22	
M44	0.15	0.5	0.35	0.24	
M45	0.15	0.5	0.35	0.26	
M46	0.15	0.4	0.45	0.22	
M47	0.15	0.4	0.45	0.24	
M48	0.15	0.4	0.45	0.26	
M49	0.2	0.7	0.1	0.22	
M50	0.2	0.7	0.1	0.24	
M51	0.2	0.7	0.1	0.26	
M52	0.2	0.6	0.2	0.22	
M53	0.2	0.6	0.2	0.24	
M54	0.2	0.6	0.2	0.26	
M55	0.2	0.5	0.3	0.22	
M56	0.2	0.5	0.3	0.24	
M57	0.2	0.5	0.3	0.26	
M58	0.2	0.4	0.4	0.22	
M59	0.2	0.4	0.4	0.24	
M60	0.2	0.4	0.4	0.26	
M61	0.3	0.6	0.1	0.22	
M62	0.3	0.6	0.1	0.24	
M63	0.3	0.6	0.1	0.26	
M64	0.3	0.5	0.2	0.22	
M65	0.3	0.5	0.2	0.24	
M66	0.3	0.5	0.2	0.26	
M67	0.3	0.4	0.3	0.22	
M68	0.3	0.4	0.3	0.24	
M69	0.3	0.4	0.3	0.26	

specimen, respectively; H (mm) represents the hydraulic head difference.

The equipment used in the permeability tests was self-made in the laboratory, and the schematic diagram is presented in Figure 4. During the test, water was injected above the steel mold, then flooded the pervious concrete specimen below, and entered the tank, while the excess water overflowed from the outlet pipe. When the flow was too large, water can flow out through the vent pipe above the steel mold. It should be noted that the water level inside the steel mold should be kept constant and then the head difference can be recorded to calculate the permeability coefficient of the specimen.

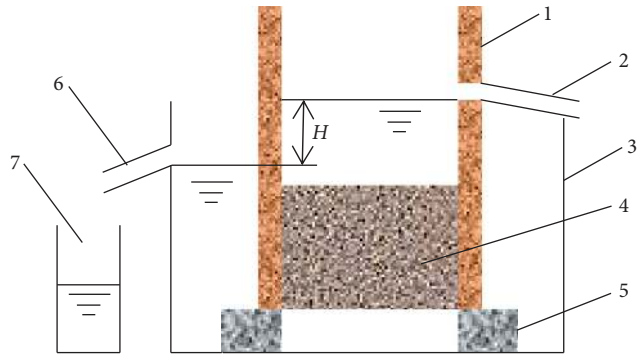

Figure 4: Schematic diagram of the permeable test device.*Notes: 1: steel mold; 2: vent pipe; 3: water tank; 4: concrete specimen; 5: pad; 6: outlet pipe; 7: measuring cylinder.

4.2. Model Validation

4.2.1. Methods for Model Validation. In the present study, the evolved random forest model was trained for the 70% dataset while the remaining 30% was for the testing dataset. It should be noted that all datasets should be split randomly during the training and validating process. Besides, two parameters (correlation, R; root-mean-square error, E_{RMS}) that were widely used in the previous studies were selected to assess the predictive ability of the dataset. The two parameters can be given as follows:

$$R = \frac{\sum_{i=1}^{N}\left(y_i^* - \overline{y^*}\right)\left(y_i - \overline{y}\right)}{\sqrt{\sum_{i=1}^{N}\left(y_i^* - \overline{y^*}\right)^2} \cdot \sqrt{\sum_{i=1}^{N}\left(y^i - \overline{y}\right)^2}},$$
$$E_{\mathrm{RMS}} = \sqrt{\frac{1}{N}\sum_{i=1}^{N}\left(y_i^* - y_i\right)^2}, \quad (2)$$

where N represents the collected numbers of the dataset; y_i and y_i^* represent actual values and predicted values, respectively; $\overline{y}$ and $\overline{y}^*$ represent the mean of the actual values and the predicted values. In addition, in order to minimize the deviation, the so-called 10-fold cross-validation method was adopted in the present study [43]. Under such a validation system, the samples as training dataset are divided into 10 subsets, one of these 10 subsets is applied to verify the predicted results of the BRF method, and the remaining 9 subsets are applied for training. Such a process should be repeated 10 times as described above.

4.2.2. Procedures of Hyperparameter Tuning. In order to obtain the optimized RF structure, hyperparameter tuning should be conducted. In the present study, the BAS algorithm was applied to tune two important parameters (the number of the trees, named as tree_num; the minimum number of samples required at a leaf node in RF, named as min_sample_leaf). Through the 10-fold cross-validation method introduced above, the 9 subsets as the training set were applied to search for the idealized hyperparameters of RF. This process should be performed 50 times by BAS [37]. For the validation dataset, the smallest E_{RMS} was selected after 50 iterations and in this fold, it can represent the optimized RF model. Consequently, the optimized RF model and the corresponding optimized hyperparameters (tree_num and min_sample_leaf) can be selected after 10 times. Due to the possibility of overfitting, the performance of the RF model should be verified by evaluating the testing set. Figure 5 summarizes the flowchart of the hyperparameters for RF tuning by BAS during training and testing.

4.2.3. Dataset Description. The dataset of pervious concrete from the experimental testing is applied to establish and validate the proposed BRF model for permeability prediction. A total of 36 mixes were used for the verification and prediction of the proposed model. It should be noted that the test results of the water permeability of each mixture are derived from the average of three parallel samples. Four key influencing variables (aggregate proportion of G_1 and G_1%; the aggregate proportion of G_2 and G_2%; the aggregate proportion of G_3 and G_3%; cement-aggregate ratio, C/A) were determined in the present study, as given in Table 3. These four variables have been confirmed in previous studies to have significant effects on the water permeability of pervious concrete and its clogging behavior [44–46]. Table 3 gives the influencing variables and their values in the design of pervious concrete, which were used to construct the dataset.

The main goal is to predict the permeability coefficient of pervious concrete, which is determined by the mix-design parameters. The relative importance of the mix-design parameters used for the input variables needs further analysis. It should be noted that the collected dataset should be normalized to [0, 1] in order to improve the efficiency of the proposed model. According to the proportion of the dataset, 25 mixes (70%) were randomly selected as the training dataset, and the other 11 mixes (30%) were used as the testing dataset (Figure 5).

5. Results and Discussion

5.1. Results of Hyperparameter Tuning. In order to obtain the optimized RF structure, the hyperparameters were adjusted on the testing set based on E_{RMS} obtained from the 10-fold

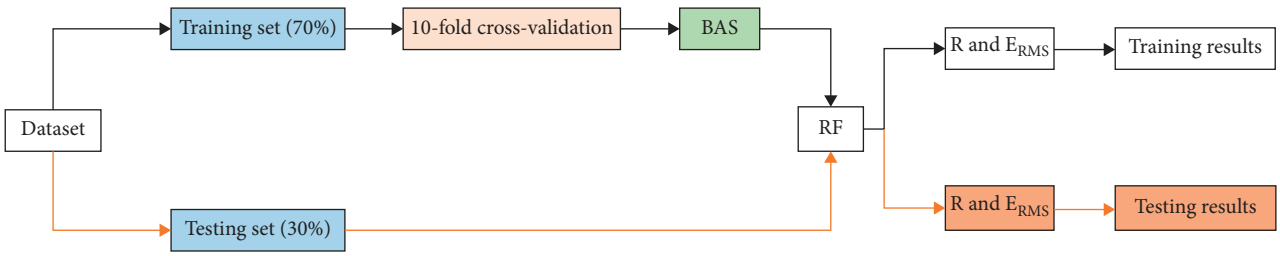

Figure 5: Flowchart of the hyperparameters for RF tuning by BAS during training and testing.

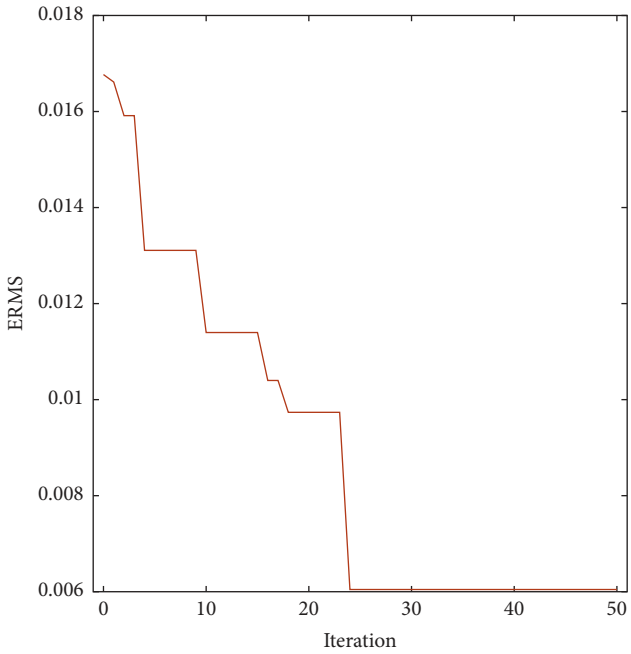

Figure 6: Relationship between the iteration and E_{RMS}.

cross-validation. Figure 6 gives the relationship between E_{RMS} and iterations during BAS tuning, which was performed 50 times in the present study.

It can be seen that E_{RMS} was greatly reduced with the increase of iteration, indicating that BAS can effectively tune the RF structure. In addition, E_{RMS} converged and reached the minimum value after 25 iterations, indicating that the optimized RF model was obtained in this fold. During the 10-fold cross-validation process, the optimized RF model in the whole calculation was determined after 10-fold and the corresponding optimized hyperparameters can be obtained. It should be noted that the prediction results of the RF should be verified through the way of evaluating the testing set. Table 4 gives the final hyperparameters of RF.

5.2. Assessing the Established Model. Figure 7 gives the comparison of the predicted permeability of the pervious concrete by the proposed method and the actual one in datasets.

Good agreement can be seen between the predicted permeability of pervious concrete and the actual

Table 4: Final hyperparameters of RF.

Parameters	Initial	Results	Empirical scope
tree_num	6	9	[1, 10]
min_sample_leaf	6	1	[1, 10]

permeability, indicating that the proposed method can well establish the nonlinear relationship between the permeability of pervious concrete and the input variables.

Furthermore, the statistical parameters of these comparisons for training and testing datasets were obtained, as shown in Table 5. The low E_{RMS} values of 0.0059 and 0.0131 can be observed for the training and testing dataset, respectively. Also, the high R values for the training set and test set were 0.9258 and 0.9208, respectively. All the above results indicated that the proposed RF model has no overfitting

5.3. Variable Importance of Pervious Concrete. Figure 8 gives the relative importance of the 4 design parameters, which were used as the input variables in the machine learning process.

Obviously, C/A was the most important design variable to determine the permeability of pervious concrete, since the highest importance score of 1.7762 can be observed. The mechanism of the effect of C/A on water permeability is that as C/A increases, the compaction resistance provided by the reduced aggregates decreases, resulting in a decrease in the volume of intercrystalline voids. This leads to lower porosity and permeability. The results of this study indicated that the effect mechanism of C/A on permeability exceeded the role of the aggregate proportion in determining permeability. Contemporaneously, the results were consistent with the findings noted by Zhang et al., Chandrappa et al., and Wang et al. [18, 47, 48]. As the largest aggregate used in the testing, the proportion of $G3$ (9.50 mm to 13.2 mm) also played an important role in determining the permeability of pervious concrete. This result was in line with the permeability properties of pervious concrete developed in the previous studies to understand the effects of aggregate sizes [44, 49, 50]. Also, it can be observed that the importance score of the $G1$ (2.36 mm–4.75 mm) aggregate is 0.8440, which ranks third among all variables by virtue of this score, indicating that it was more sensitive than the $G2$ (4.75 mm–9.50 mm) aggregate in determining the permeability of pervious

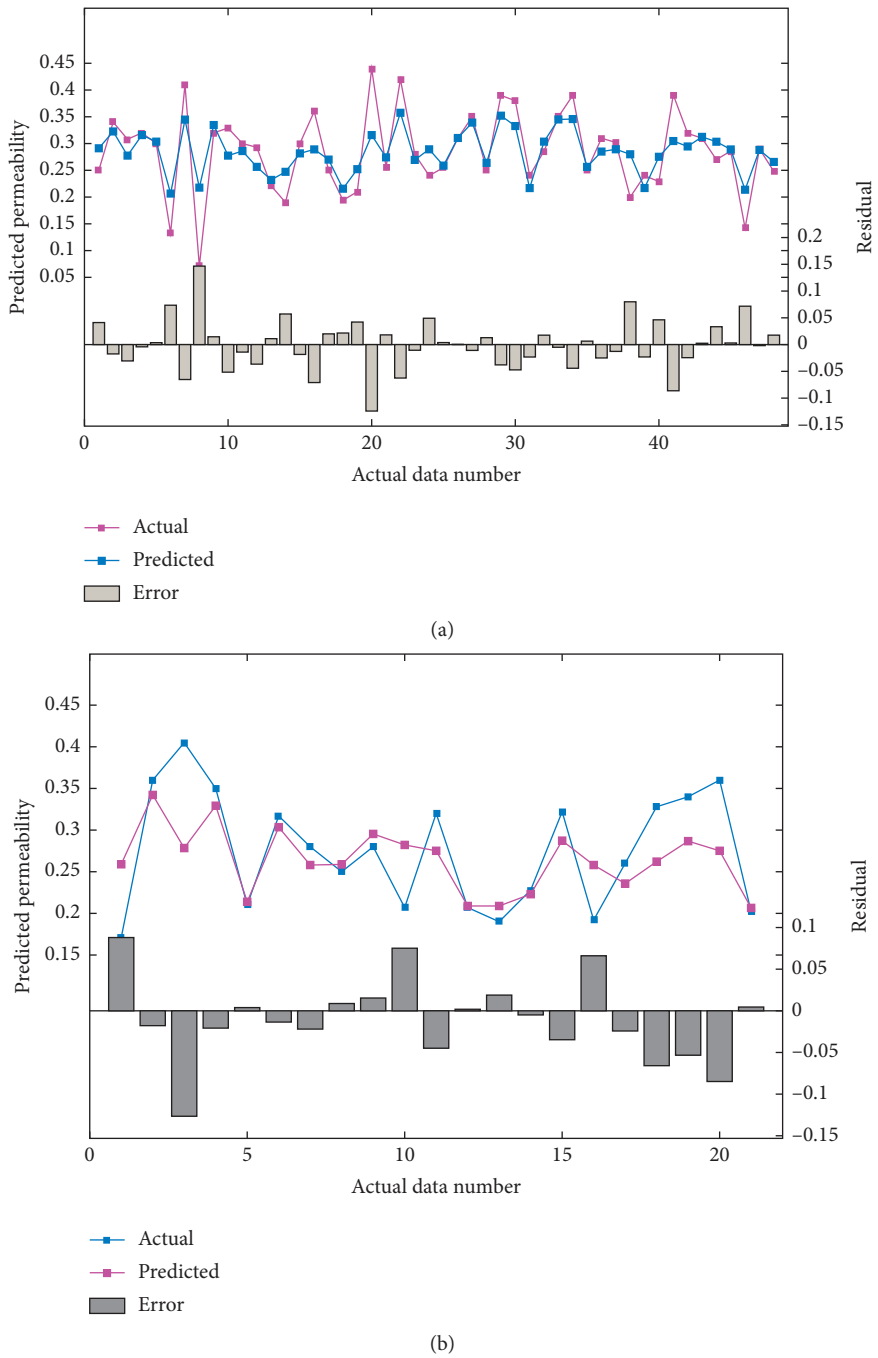

Figure 7: Comparison of permeability. (a) Training dataset. (b) Testing dataset.

Table 5: Statistical parameters of actual and predicted permeability in the datasets.

Datasets	E_{RMS}	R
Training dataset	0.0059	0.9258
Testing dataset	0.0131	0.9208

concrete. Therefore, in the future tests of pervious concrete, more C/A and $G3$ aggregate proportion combinations should be selected to optimize the target permeability. The results obtained can effectively guide the design of pervious concrete and select appropriate parameters to optimize C/A and aggregate gradation.

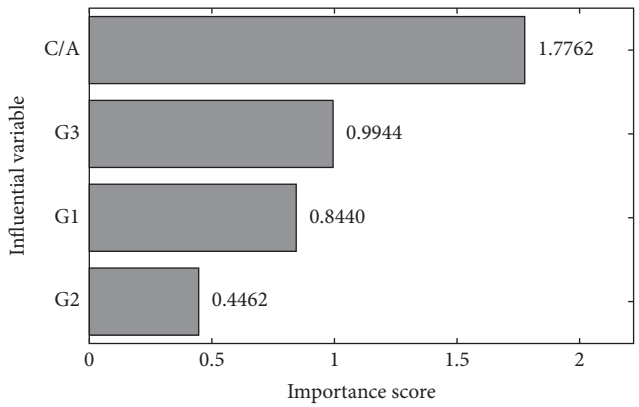

Figure 8: Importance score of the four design parameters.

6. Conclusions

The present study aims to propose a method to combine the beetle antennae search (BAS) and random forest (RF) algorithm to predict the permeability of pervious concrete. Based on the 36 samples designed in the laboratory and 4 key influencing variables, the permeability of pervious concrete can be determined by the independent variables under the RF model. The BAS algorithm was used to tune the hyperparameters of RF and the results were verified by 10-fold cross-validation. The prediction results of the optimized BRF were evaluated through R and E_{RMS}. The importance of the variables that determine permeability is also revealed and discussed. The following are the conclusions drawn from the above research process:

(i) The BAS algorithm is effective for adjusting the hyperparameters of RF and can be applied in evolved RF to construct predictive models; it has higher reliability and effectiveness than random hyperparameter selection.

(ii) The proposed RF model can accurately predict the permeability of pervious concrete, which can guide the functional designing for pervious concrete; for the testing set, R and E_{RMS} were 0.9223 and 0.0123, respectively, indicating that the proposed RF model showed good predictive ability on the collected dataset.

(iii) The C/A (cement/aggregate ratio) can be considered as the most significant variable for determining the permeability of pervious concrete, followed by the coarse aggregate proportions. Among them, the proportion of $G3$ and $G1$ aggregates is considered to be the most significant variable affecting the permeability for pervious concrete. However, the proportion of $G2$ aggregate has an almost negligible influence on the permeability. The results obtained can effectively guide the design of pervious concrete and select appropriate parameters to optimize C/A and aggregate gradation.

It should be noted that the results obtained in this study were limited by the number of samples. If more datasets and more variables are considered, the predicted permeability closer to the actual ones can be obtained. In the future, more samples with different combinations will be designed, mixed, and tested to obtain larger data sets for analysis through machine learning methods to more widely and effectively apply pervious concrete in the field of green construction.

Data Availability

The data used to support the findings of this study are available from the corresponding author upon request.

Conflicts of Interest

There are no conflicts of interest.

Authors' Contributions

Jiandong Huang and Yi Zhang contributed to conceptualization; Jiandong Liu and Jiandong Huang contributed to methodology; Jiandong Huang, Yi Zhang, and Lin Wang wrote the original draft; Tianhong Duan and Yawei Lei reviewed and edited the article; Tianhong Duan supervised the study. All authors have read and agreed to the published version of the manuscript.

Acknowledgments

The authors sincerely acknowledge the support from Independent Research Projects of State Key Laboratory of Coal Resources and Safe Mining, China University of Mining and Technology (SKLCRSM18X013).

References

[1] L. Haselbach, V. F. P. Dutra, P. Schwetz, and L. C. P. da Silva Filho, "Laboratory evaluations of long-term hydraulic performance and maintenance requirements for pervious concrete mixes: A case study in Southern Brazil," in *Proceedings of the International Conference on Transportation and Development*, vol. 2016, pp. 309–317, Houston, TX, USA, June 2016.

[2] J. Sanslone, X. Kuang, and V. Ranieri, "Permeable pavement as a hydraulic and filtration interface for urban drainage," *Journal of Irrigation and Drainage Engineering*, vol. 134, pp. 666–674, 2008.

[3] M. S. Sumanasooriya and N. Neithalath, "Stereology-and morphology-based pore structure descriptors of enhanced porosity (pervious) concretes," *ACI Materials Journal*, vol. 106, 2009.

[4] J. Huang, R. Alyousef, M. Suhatril, S. Baharom et al., "Influence of porosity and cement grade on concrete mechanical properties," *Advances in Concrete Construction*, vol. 10, no. 5, pp. 393–402, 2011.

[5] L. Haselbach, M. Boyer, J. T. Kevern, and V. R. Schaefer, "Cyclic heat island impacts on traditional versus pervious concrete pavement systems," *Transportation Research Record: Journal of the Transportation Research Board*, vol. 2240, no. 1, pp. 107–115, 2011.

[6] A. Mohajerani, J. Bakaric, and T. Jeffrey-Bailey, "The urban heat island effect, its causes, and mitigation, with reference to

the thermal properties of asphalt concrete," *Journal of Environmental Management*, vol. 197, pp. 522–538, 2017.

[7] Y. Qin, H. Yang, Z. Deng, and J. He, "Water permeability of pervious concrete is dependent on the applied pressure and testing methods," *Advances in Materials Science and Engineering*, vol. 2015, Article ID 404136, 6 pages, 2015.

[8] Y. Zhang, H. Li, A. Abdelhady, and H. Du, "Laboratorial investigation on sound absorption property of porous concrete with different mixtures," *Construction and Building Materials*, vol. 259, p. 120414, 2020.

[9] Y. Zhang, H. Li, A. Abdelhady, and J. Yang, "Effect of different factors on sound absorption property of porous concrete," *Transportation Research Part D: Transport and Environment*, vol. 87, p. 102532, 2020.

[10] J. Huang, J. Zhang, J. Ren, and H. Chen, "Anti-rutting performance of the damping asphalt mixtures (DAMs) made with a high content of asphalt rubber (AR)," *Construction and Building Materials*, vol. 271, Article ID 121878, 2020 In press.

[11] P. D. Tennis, M. L. Leming, and D. J. Akers, *Pervious Concrete Pavements*, Portland Cement Association Skokie, Skokie, IL, USA, 2004.

[12] P. Chindaprasirt, S. Hatanaka, T. Chareerat, N. Mishima, and Y. Yuasa, "Cement paste characteristics and porous concrete properties," *Construction and Building Materials*, vol. 22, no. 5, pp. 894–901, 2008.

[13] M. S. Sumanasooriya and N. Neithalath, "Pore structure features of pervious concretes proportioned for desired porosities and their performance prediction," *Cement and Concrete Composites*, vol. 33, no. 8, pp. 778–787, 2011.

[14] A. K. Chandrappa and K. P. Biligiri, "Pervious concrete as a sustainable pavement material - research findings and future prospects: a state-of-the-art review," *Construction and Building Materials*, vol. 111, pp. 262–274, 2016.

[15] J. Huang and Y. Sun, "Effect of modifiers on the rutting, moisture-induced damage, and workability properties of hot mix asphalt mixtures," *Applied Sciences*, vol. 10, no. 20, p. 7145, 2020.

[16] J. Huang and Y. Sun, "Viscoelastic analysis of the damping asphalt mixtures (dams) made with a high content of asphalt rubber (ar)," *Advances in Civil Engineering*, vol. 2020, Article ID 8826926, 12 pages, 2020.

[17] F. Montes, S. Valavala, and L. M. Haselbach, "A new test method for porosity measurements of portland cement pervious concrete," *Journal of ASTM International*, vol. 2, pp. 1–13, 2005.

[18] H. Wang, H. Li, X. Liang, H. Zhou, N. Xie, and Z. Dai, "Investigation on the mechanical properties and environmental impacts of pervious concrete containing fly ash based on the cement-aggregate ratio," *Construction and Building Materials*, vol. 202, pp. 387–395, 2019.

[19] A. Torres, J. Hu, and A. Ramos, "The effect of the cementitious paste thickness on the performance of pervious concrete," *Construction and Building Materials*, vol. 95, pp. 850–859, 2015.

[20] K. Cosic, L. Korat, V. Ducman, and I. Netinger, "Influence of aggregate type and size on properties of pervious concrete," *Construction and Building Materials*, vol. 78, pp. 69–76, 2015.

[21] X. Kuang, J. Sansalone, G. Ying, and V. Ranieri, "Pore-structure models of hydraulic conductivity for permeable pavement," *Journal of Hydrology*, vol. 399, no. 3-4, pp. 148–157, 2011.

[22] R. Zhong, M. Xu, R. Vieira Netto, and K. Wille, "Influence of pore tortuosity on hydraulic conductivity of pervious concrete: characterization and modeling," *Construction and Building Materials*, vol. 125, pp. 1158–1168, 2016.

[23] K. Xie, Y. Du, and C. Sun, "Application of the mind-evolution-based machine learning in mixture-ratio calculation of raw materials cement," in *Proceedings of the 3rd World Congress on Intelligent Control and Automation (Cat. No. 00EX393)*, pp. 132–134, IEEE, Hefei, China, July 2000.

[24] G. Ozcan, Y. Kocak, and E. Gulbandilar, "Estimation of compressive strength of bfs and wtrp blended cement mortars with machine learning models," *Computers and Concrete*, vol. 19, no. 3, pp. 275–282, 2017.

[25] A. Shadravan, M. Tarrahi, and M. Amani, "intelligent cement design: utilizing machine learning algorithms to assure effective long-term well integrity," in *Proceedings of the Carbon Management Technology Conference*, Sugarland, TX, USA, November 2015.

[26] A. Shadravan, M. Tarrahi, and M. Amani, "Intelligent tool to design fracturing, drilling, spacer and cement slurry fluids using machine learning algorithms," in *Proceedings of the SPE Kuwait Oil and Gas Show and Conference*, Society of Petroleum Engineers, Mishref, Kuwait, October 2015.

[27] T. Oey, S. Jones, J. W. Bullard, and G. Sant, "Machine learning can predict setting behavior and strength evolution of hydrating cement systems," *Journal of the American Ceramic Society*, vol. 103, no. 1, pp. 480–490, 2020.

[28] A. Menon, C. M. Childs, B. Poczos, N. R. Washburn, and K. E. Kurtis, "Molecular engineering of superplasticizers for metakaolin-portland cement blends with hierarchical machine learning," *Advanced Theory and Simulations*, vol. 2, no. 4, p. 1800164, 2019.

[29] N.-D. Hoang, C.-T. Chen, and K.-W. Liao, "Prediction of chloride diffusion in cement mortar using multi-gene genetic programming and multivariate adaptive regression splines," *Measurement*, vol. 112, pp. 141–149, 2017.

[30] G. Konstantopoulos, E. P. Koumoulos, and C. A. Charitidis, "Testing novel portland cement formulations with carbon nanotubes and intrinsic properties revelation: nano-indentation analysis with machine learning on microstructure identification," *Nanomaterials*, vol. 10, no. 4, p. 645, 2020.

[31] J. Huang, P. G. Asteris, S. M. K. Pasha, A. S. Mohammed, and M. Hasanipanah, "A new auto-tuning model for predicting the rock fragmentation: a cat swarm optimization algorithm," *Engineering with Computers*, pp. 1–12, 2020.

[32] J. Huang, M. Koopialipoor, and D. J. Armaghani, "A combination of fuzzy delphi method and hybrid ann-based systems to forecast ground vibration resulting from blasting," *Scientific Reports*, vol. 10, p. 19397, 2020.

[33] N.-D. Hoang, "Estimating punching shear capacity of steel fibre reinforced concrete slabs using sequential piecewise multiple linear regression and artificial neural network," *Measurement*, vol. 137, pp. 58–70, 2019.

[34] S. M. Jamal, N. Deshpande, and S. Londhe, "Predicting strength of recycled aggregate concrete using artificial neural network, adaptive neuro-fuzzy inference system and multiple linear regression," *International Journal of Sustainable Built Environment*, vol. 5, pp. 355–369, 2016.

[35] F. Khademi, M. Akbari, S. M. Jamal, and M. Nikoo, "Multiple linear regression, artificial neural network, and fuzzy logic prediction of 28 days compressive strength of concrete," *Frontiers of Structural and Civil Engineering*, vol. 11, no. 1, pp. 90–99, 2017.

[36] V. Nilsen, L. T. Pham, M. Hibbard, A. Klager, S. M. Cramer, and D. Morgan, "Prediction of concrete coefficient of thermal expansion and other properties using machine learning,"

Construction and Building Materials, vol. 220, pp. 587–595, 2019.

[37] Y. Sun, G. Li, J. Zhang, and D. Qian, "Prediction of the strength of rubberized concrete by an evolved random forest model," *Advances in Civil Engineering*, vol. 2019, Article ID 5198583, 7 pages, 2019.

[38] X. Jiang and S. Li, "BAS: beetle antennae search algorithm for optimization problems," 2017, http://arxiv.org/abs/1710.10724.

[39] T. Joshi and U. Dave, "Evaluation of strength, permeability and void ratio of pervious concrete with changing w/c ratio and aggregate size," *International Journal of Civil Engineering and Technology*, vol. 7, pp. 276–284, 2016.

[40] Z. Dai, H. Li, W. Zhao et al., "Multi-modified effects of varying admixtures on the mechanical properties of pervious concrete based on optimum design of gradation and cement-aggregate ratio," *Construction and Building Materials*, vol. 233, p. 117178, 2020.

[41] N. Neithalath, *Development And Characterization Of Acoustically Efficient Cementitious Materials*, Portland Cement Association, Newyork, NY, USA, 2004.

[42] F. Imai and N. Shinnishi, *Permeability of No-Fines Concrete*, 1998.

[43] J. Sun, J. Zhang, Y. Gu, Y. Huang, Y. Sun, and G. Ma, "Prediction of permeability and unconfined compressive strength of pervious concrete using evolved support vector regression," *Construction and Building Materials*, vol. 207, pp. 440–449, 2019.

[44] A. K. Chandrappa and K. P. Biligiri, "Comprehensive investigation of permeability characteristics of pervious concrete: a hydrodynamic approach," *Construction and Building Materials*, vol. 123, pp. 627–637, 2016.

[45] A. A. Aliabdo, A. E. M. Abd Elmoaty, and A. M. Fawzy, "Experimental investigation on permeability indices and strength of modified pervious concrete with recycled concrete aggregate," *Construction and Building Materials*, vol. 193, pp. 105–127, 2018.

[46] B. Huang, H. Wu, X. Shu, and E. G. Burdette, "Laboratory evaluation of permeability and strength of polymer-modified pervious concrete," *Construction and Building Materials*, vol. 24, no. 5, pp. 818–823, 2010.

[47] Y. Zhang, H. Li, A. Abdelhady, and J. Yang, "Comparative laboratory measurement of pervious concrete permeability using constant-head and falling-head permeameter methods," *Construction and Building Materials*, vol. 263, p. 120614, 2020.

[48] A. K. Chandrappa and K. P. Biligiri, "Effect of pore structure on fatigue of pervious concrete," *Road Materials and Pavement Design*, vol. 20, pp. 1525–1547, 2019.

[49] S. O. Ekolu, S. Diop, and F. Azene, "Properties of pervious concrete for hydrological applications," *Concrete Beton*, vol. 144, pp. 18–25, 2016.

[50] H. Liu, G. Luo, H. Wei, and H. Yu, "Strength, permeability, and freeze-thaw durability of pervious concrete with different aggregate sizes, porosities, and water-binder ratios," *Applied Sciences*, vol. 8, no. 8, p. 1217, 2018.